Vol 18 No 2, February 2009
1674-1056/2009/18(02)/0773-05

Chinese Physics B

© 2009 Chin. Phys. Soc.
and IOP Publishing Ltd

Columnar growth of crystalline silicon films on aluminium-coated glass by inductively coupled plasma CVD at room temperature*

Wang Jin-Xiao(王金晓), Qin Yan-Li(秦艳丽), Yan Heng-Qing(闫恒庆), Gao Ping-Qi(高平奇), Li Jun-Shuai(栗军帅), Yin Min(尹 旻), and He De-Yan(贺德衍)†

Department of Physics, Lanzhou University, Lanzhou 730000, *China*

(Received 1 July 2008; revised manuscript received 22 July 2008)

Silicon films were grown on aluminium-coated glass by inductively coupled plasma CVD at room temperature using a mixture of SiH_4 and H_2 as the source gas. The microstructure of the films was evaluated using Raman spectroscopy, scanning electron microscopy and atomic force microscopy. It was found that the films are composed of columnar grains and their surfaces show a random and uniform distribution of silicon nanocones. Such a microstructure is highly advantageous to the application of the films in solar cells and electron emission devices. Field electron emission measurement of the films demonstrated that the threshold field strength is as low as $\sim 9.8\,\mathrm{V}/\mu\mathrm{m}$ and the electron emission characteristic is reproducible. In addition, a mechanism is suggested for the columnar growth of crystalline silicon films on aluminium-coated glass at room temperature.

Keywords: surface structure, columnar growth, inductively coupled plasma CVD, crystalline silicon films

PACC: 7360F, 7830G, 7970, 8115H

1. Introduction

There has been an increasing interest in preparation of low-temperature crystalline silicon films due to their potential applications in developing new technologies including inexpensive flexible electronics, solar cells, thin film transistor arrays of liquid crystal displays and imaging sensors.[1,2] Solid phase crystallization of amorphous silicon (a-Si) film is a common method to prepare crystalline silicon films. However, the crystallization temperature is too high to use glass or plastic substrates.[3−5] Liquid-phase crystallization of a-Si films on glass substrates using excimer lasers has been intensively investigated, but the thickness for crystallization is less than 100 nm due to the high absorption coefficient of a-Si for the lasers used.[6]

Many efforts have been made to directly grow crystalline silicon films at low temperatures. Although crystalline silicon films can be deposited on glass by plasma-enhanced chemical vapour deposition,[7,8] the substrate temperature is still too high for the use of low-temperature substrates such as the plastic. Moreover, the deposition rate is low. To decrease the substrate temperature and increase the deposition rate of crystalline silicon films, various plasma sources have been developed, including electron cyclotron resonance, surface wave plasma, and inductively coupled plasma (ICP).[9−12] Of these plasma sources, ICP has some advantages in the deposition of low-temperature crystalline silicon films: low plasma potential, low electron temperature, high electron density ($\sim 10^{12}\,\mathrm{cm}^{-3}$ at 10 mTorr) (1 Torr = 133 Pa), spatial confinement of discharge and the simplicity of the configuration.[13−15]

In this paper, the ICP-CVD technique was employed to directly deposit crystalline Si films on aluminium-coated glass at room temperature. The thickness of the evaporated aluminium layer is about 100 nm. A mixture of SiH_4 and H_2 was used as the source gas. The microstructure of the samples was characterized by micro-Raman spectroscopy, scanning electron microscopy (SEM) and atomic force microscopy (AFM). The results show that the resulting crystalline silicon film has high-density silicon tips

*Project supported by the National Natural Science Foundation of China (Grant No 60776009).
†Corresponding author. E-mail: hedy@lzu.edu.cn

with a random distribution on the surface and columnar growth in the film. The field emission measurement suggests that the samples have good field emission characteristics.

2. Experimental details

The plasma was generated by a built-in water-cooled one-turn induction coil (10 cm in diameter) made of a copper tube inside the reactor. In order to obtain high-density and homogeneous plasma, the surface of the induction coil was coated with a layer of 0.1 cm thick fiberglass as an insulator. The base vacuum was 1×10^{-3} Pa and the working pressure was about 10 Pa. The SiH_4 dilution ratio ($[SiH_4]/([SiH_4]+[H_2])$) was fixed at 10%. The radio-frequency power was 300 W. As the substrates were not completely immersed in the plasma, the measured substrate temperature was only about 40 °C under plasma heating even at an input power of 300 W.

The field emission measurements were conducted under a vacuum below 1.0×10^{-3} Pa in a high-vacuum setup.

3. Results and discussion

The Raman spectra of the silicon films deposited on bare and aluminium-coated glass are shown in Fig.1. The broad band centred at 480 cm^{-1}, corresponding to the transverse optical phonon scattering of amorphous silicon, shows that the structure of the film deposited on bare glass is amorphous. In comparison, the strong Raman peak at 512 cm^{-1} for the film deposited on aluminium-coated glass shows that the aluminium layer significantly enhances the crystallization of silicon film at room temperature.

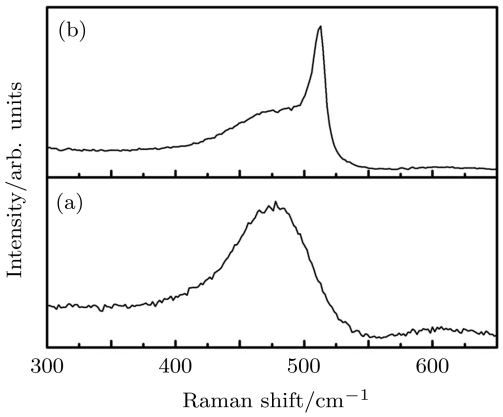


Fig.1. Raman spectra of silicon films deposited on bare (a) and aluminium-coated (b) glass.

To obtain more microstructural information for the obtained silicon films, SEM and AFM measurements were performed. Figure 2(a) shows the surface image. It can be seen that the grain size is uniform and is about 140 nm in the lateral direction. The cross-sectional SEM image (in Fig.2(b)) shows that the columnar growth predominates for the silicon film deposited on the aluminium-coated glass. Figure 3 shows the typical 2D and 3D AFM images of the silicon film deposited on the aluminium-coated glass substrate. It can be seen that the film surface presents a random and uniform distribution of silicon nanocones as the result of the columnar growth. The height and the mean basal diameter of these cones are ∼140 nm and ∼ 150 nm, respectively, causing a relatively high surface roughness (RMS ∼44 nm).

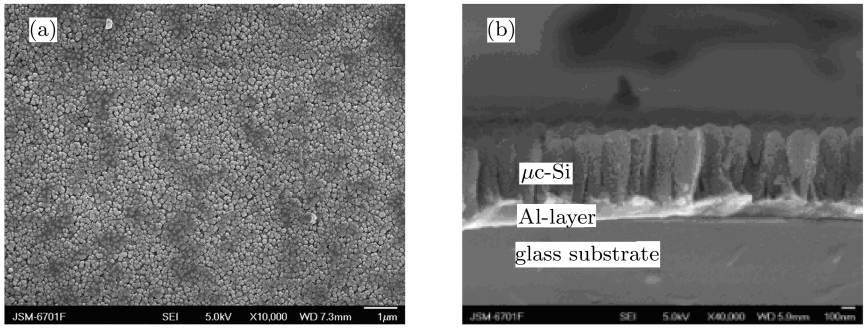


Fig.2. Surface (a) and cross-sectional (b) SEM images of the silicon film deposited on aluminium-coated glass.

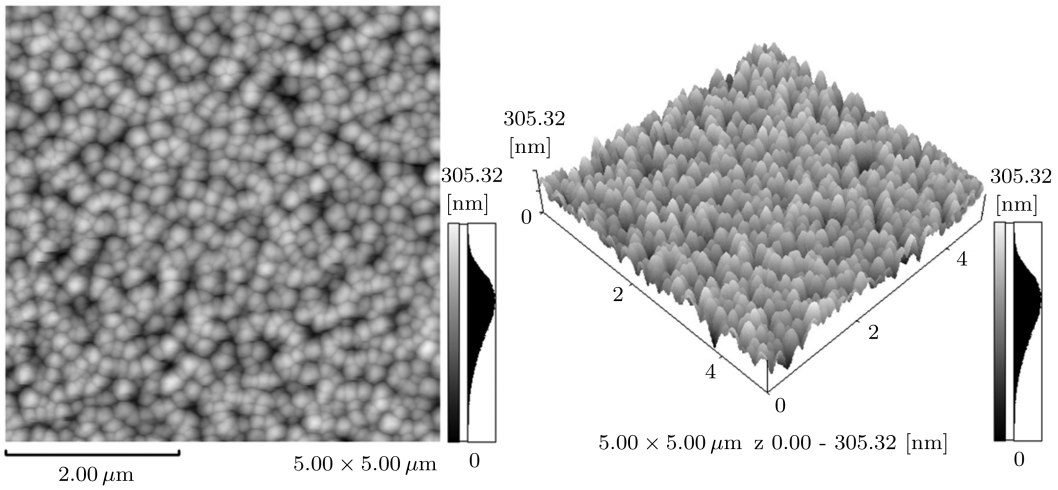


Fig.3. Typical 2D and 3D AFM images of the silicon film deposited on aluminium-coated glass.

It is well known that the recrystallization temperature of amorphous silicon films can be effectively decreased by making them in contact with some metals such as Al or Au, which is called metal-induced annealing crystallization.[16−20] Normally, the crystallization temperature of amorphous silicon films is about 500 °C in Al-induced annealing crystallization processes. Our results indicate that the crystallization temperature of silicon films can be further decreased by Al-induced crystallization in the ICP-CVD process. Here we make the tentative assumption that the reduced crystallization temperature is due to the difference in the ways of supply of silicon atoms in the traditional annealing process and the Al-induced crystallization growth process in ICP-CVD. Meanwhile, the strong nonequilibrium chemical processes caused by the high-density electrons in ICP also play an important role in decreasing the induced crystallization temperature. Our reasoning is as follows.

In the traditional Al-induced annealing crystallization process, silicon atoms that diffuse into Al layer and recrystallize, come from the breaking of Si-Si bonds in amorphous silicon with the assistance of the Al layer.[21] Although the existence of the Al layer can decrease the crystallization temperature, it still needs higher temperature to activate the Si-Si bonds to break. However, in ICP-CVD process, the silicon atoms are provided by high energy state SiH_x ($0 \leq x \leq 3$) radicals created by plasma stimulation, which effectively reduces the crystallization temperature.

With the continuous dissolution of silicon atoms, the silicon concentration in Al exceeds the saturation value. They will precipitate from the aluminium lattice and nucleate in the low-energy sites, such as the aluminium grain boundaries or the surface of the aluminium layer, as shown in Fig.4. The grains which nucleate in the aluminium grain boundaries will stop growing when the grains touch the upper and lower surfaces of the aluminium layer. The silicon grains which have nucleated on the surface of the aluminium layer will continue to grow in the direction of the normal of the upper surface of the aluminium layer as silicon atoms accumulate at the bottom of the silicon grains, leading to the columnar structure of the resultant silicon film as shown in Fig.2. Such a growth process is schematically demonstrated in Fig.4.

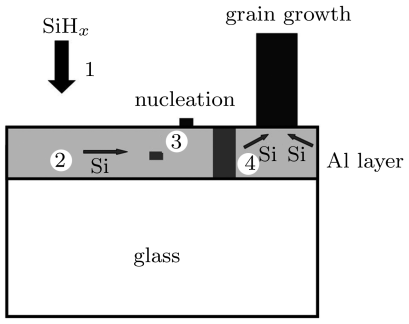


Fig.4. Schematic diagram of Al-induced growth of crystalline silicon films by ICP-CVD: (1) diffusion of SiH_x ($0 \leq x \leq 3$) to the substrate; (2) diffusion of silicon atoms in the aluminium layer; (3) nucleation of silicon atoms; (4) growth of silicon grains.

The films with the microstructure as shown in Figs.2 and 3 are highly advantageous to the applications in solar cells and electron emission devices. To check the electron emission characteristic of the film

deposited on the aluminium-coated glass substrate, we measured the field electron emission from 0 to 1000 V. The crystalline silicon film on aluminium-layer served as a cathode and the distance between the anode and the cathode was fixed at 50 μm using a glass spacer. The measurement was performed repeatedly at a pressure below 1.0×10^{-3} Pa. The J–E curves obtained are shown in Fig.5. The typical threshold field strength, which is defined as the macroscopic field to

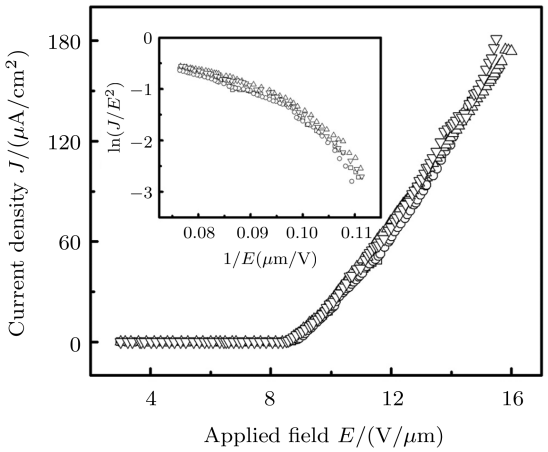


Fig.5. Field emission characteristics of the silicon film deposited on aluminium-coated glass. The corresponding F-N curve is plotted in the inset.

detect a current density of 20 μA/cm^2, is about 9.8 V/μm, which is considerably lower than that ($\sim$ 20 Vμm^{-1}) observed for conventional micro-fabricated silicon materials.[22] This could be attributed to the random and uniform distribution of silicon nanocones on the surface and the columnar microstructure of the film. More importantly, there was no distinct change of the J–E curves measured at different times, suggesting that the sample has a stable field electron emission performance. The F-N plot shown in the inset of Fig.5 is in agreement with the F-N theory, from which the slope of the F-N plot, S, can be expressed as

$$S = \frac{-B\phi^{3/2}}{\beta},$$

where B is a constant having the value 6.831×10^3 eV$^{-3/2}$Vμm^{-1}, ϕ is the effective work function (being about 4.15 eV for silicon),[23] β is the field enhancement factor. In our case, the calculated β is about 1136. Thus, the shape of the surface humps of silicon crystallites on the aluminium-coated glass might be the reason of the lowered threshold voltage compared to bulk silicon.

4. Conclusions

In summary, we have deposited silicon films on aluminium-coated glass at room temperature by ICP-CVD. The films are composed of columnar grains and the lateral grain size is about 140 nm. The 3D AFM images show that silicon nanocones are randomly and uniformly distributed on the film surface. The height and mean basal diameter of the silicon nanocones are about 140 and 150 nm, respectively. The field electron emission measurement shows that the silicon films deposited on the aluminium-coated glass have low threshold field strength of about 9.8 V/μm, resulting from the random and uniform distribution of silicon nanocones on the film surface and the columnar microstructure in the films. Moreover, the field electron emission characteristic is reproducible.

References

[1] Sposili R S and Im J S 1996 *Appl. Phys. Lett.* **69** 2864
[2] Eldin H and Elgamel A 1998 *Sol. Energy Mater. Sol. Cells* **53** 277
[3] Inversion R B and Rief R 1987 *J. Appl. Phys.* **62** 1675
[4] Schaber H, Cutter D, Binder J and Obermeier E 1993 *J. Appl. Phys.* **54** 4633
[5] Dai M, Zhang L, Bao Y, Shi J J, Chen K, Li W, Huang X F and Chen K J 2002 *Chin. Phys.* **11** 944
[6] Sameshima T, Hara M and Usui S 1989 *Jpn. J. Appl. Phys.* **28** 1789
[7] Sugai H, Nakamura K and Suzuki K 1994 *Jpn. J. Appl. Phys.* **33** 2189
[8] Zhang X D, Zhao Y, Zhu F, Sun J, Wei C C, Hou G F, Geng X H and Xiong S Z 2004 *Chin. Phys.* **13** 1370
[9] Sieber I, Wanderka N, Kaiser I and Fuhs W 2002 *Thin Solid Films* **403-404** 543
[10] Daigil C, Shin J H, Hyuk I and Han M K 2004 *Appl. Phys. Lett.* **84** 1287
[11] He D Y 2001 *Acta Phys. Sin.* **50** 779 (in Chinese)
[12] Won S H, Youn J H, Jiang J and Moon B Y 2001 *J. Korean Phys. Soc.* **39** 123
[13] Moon B Y, Youn J H, Won S H and Jang J 2001 *Sol. Energy Mater. Sol. Cells* **69** 139
[14] Mani R C, Pavel I and Aydil E S 2007 *J. Appl. Phys.* **102** 043305

[15] Li J S, Wang J X, Yin M, Gao P Q, He D Y, Chen Q, Li Y L and Shirai H 2008 *J. Appl. Phys.* **103** 043505
[16] Haque M, Naseem H and Brown W 1994 *J. Appl. Phys.* **75** 3928
[17] Pereira L, Aguas H, Martins R M, Fortunato E and Martins R 2004 *J. Non-Cryst. Solids* **338–340** 178–182
[18] Chen Y K, Lin K X, Luo Z, Liang R S and Zhou P F 2004 *Acta Phys. Sin.* **53** 582 (in Chinese)
[19] Antesberger V, Jaeger C and Stutzmann M 2008 *Journal of Non-crystalline Solids* **354** 2324
[20] Knaepen W, Detavernier C, Meirhaeghe R L V, Sweet J J and Lavoie C 2008 *Thin Solid Films* **516** 4946
[21] Schneider J, Klein J, Muske M, Gall S and Fuhs W 2005 *Appl. Phys. Lett.* **87** 031905
[22] Sugino T, Kawasaki S, Tanioka K and Shirafuji J 1997 *Appl. Phys. Lett.* **71** 2704
[23] Wang Q, Li J J, Ma Y J, Bai X D, Wang Z L, Xu P, Shi C Y, Quan B G, Yue S L and Gu C Z 2005 *Nanotechnology* **16** 2919